NATIONAL BUREAU OF STANDARDS REPORT

8991

PROCEDURES FOR PRECISE DETERMINATION
OF THERMAL RADIATION PROPERTIES

PROGRESS REPORT No. 27

May 1, 1965 - July 31, 1965

RESEARCH AND TECHNOLOGY DIVISION
UNITED STATES AIR FORCE
WRIGHT-PATTERSON AIR FORCE BASE, OHIO

U.S. DEPARTMENT OF COMMERCE
NATIONAL BUREAU OF STANDARDS

THE NATIONAL BUREAU OF STANDARDS

The National Bureau of Standards is a principal focal point in the Federal Government for assuring maximum application of the physical and engineering sciences to the advancement of technology in industry and commerce. Its responsibilities include development and maintenance of the national standards of measurement, and the provisions of means for making measurements consistent with those standards; determination of physical constants and properties of materials; development of methods for testing materials, mechanisms, and structures, and making such tests as may be necessary, particularly for government agencies; cooperation in the establishment of standard practices for incorporation in codes and specifications; advisory service to government agencies on scientific and technical problems; invention and development of devices to serve special needs of the Government; assistance to industry, business, and consumers in the development and acceptance of commercial standards and simplified trade practice recommendations; administration of programs in cooperation with United States business groups and standards organizations for the development of international standards of practice; and maintenance of a clearinghouse for the collection and dissemination of scientific, technical, and engineering information. The scope of the Bureau's activities is suggested in the following listing of its four Institutes and their organizational units.

Institute for Basic Standards. Applied Mathematics. Electricity. Metrology. Mechanics. Heat. Atomic Physics. Physical Chemistry. Laboratory Astrophysics.* Radiation Physics. Radio Standards Laboratory:* Radio Standards Physics; Radio Standards Engineering. Office of Standard Reference Data.

Institute for Materials Research. Analytical Chemistry. Polymers. Metallurgy. Inorganic Materials. Reactor Radiations. Cryogenics.* Materials Evaluation Laboratory. Office of Standard Reference Materials.

Institute for Applied Technology. Building Research. Information Technology. Performance Test Development. Electronic Instrumentation. Textile and Apparel Technology Center. Technical Analysis. Office of Weights and Measures. Office of Engineering Standards. Office of Invention and Innovation. Office of Technical Resources. Clearinghouse for Federal Scientific and Technical Information.**

Central Radio Propagation Laboratory.* Ionospheric Telecommunications. Tropospheric Telecommunications. Space Environment Forecasting. Aeronomy.

---

* Located at Poulder, Colorado 80301.

** Located at 5285 Port Royal Road, Springfield, Virginia 22171.

NATIONAL BUREAU OF STANDARDS REPORT

NBS PROJECT
21211-11-2120481

NBS REPORT
8991

PROCEDURES FOR PRECISE DETERMINATION
OF THERMAL RADIATION PROPERTIES

PROGRESS REPORT No. 27

May 1, 1965 - July 31, 1965

Contract No. DO (33-615)65-1005
Task No. 62405514

to

RESEARCH AND TECHNOLOGY DIVISION
UNITED STATES AIR FORCE
WRIGHT-PATTERSON AIR FORCE BASE, OHIO

IMPORTANT NOTICE

NATIONAL BUREAU OF STAN
for use within the Government. Be
and review. For this reason, the p
whole or in part, is not authorize
Bureau of Standards, Washington,
the Report has been specifically pr

Approved for public release by the director of the National Institute of Standards and Technology (NIST) on October 9, 2015

accounting documents intended
ijected to additional evaluation
ting of this Report, either in
ffice of the Director, National
ne Government agency for which
es for its own use.

U.S. DEPARTMENT OF COMMERCE

NATIONAL BUREAU OF STANDARDS

I. SUMMARY

Specimens of alumina, thoria, magnesia and zirconia were prepared for measurement of total normal emittance by the center post and deep cavity methods. Specimens of boron nitride were prepared for measurement by the shallow cavity method. Graphite susceptors were prepared for use with the center post and deep cavity methods.

The equations used for computing diffuse radiant heat transfer have been expressed in terms of vectors and transformations in a finite dimensional vector space. The equations can be written very compactly in this form, and certain theorems can be used to simplify the computations.

A computer code for calculating the temperature distribution in a specimen is being perfected. This code should be capable of computing the thermal gradients in the shallow cavity, graphite post and deep cavity specimens. In this code the geometric view factors are computed automatically; this permits the dimensions of the specimen, cavity and post to be varied easily.

The design of the laser-source integrating sphere reflectometer has been modified to eliminate errors due to flux reflected by the specimen impinging directly on the detector, and to permit operation in the comparison mode. A radio-frequency heater was designed to heat specimens to temperatures in the 1800-2500°K range.

II. SHALLOW CAVITY PROCEDURE FOR MEASURING TOTAL NORMAL EMITTANCE OF NONMETALS AT TEMPERATURES ABOVE 1800°K.

1. Background. Tests described in the last quarterly report indicated that measurements on a specimen of alumina were in error by about +51 percent. An error analysis indicated that there was an error of about -8.5 percent due to the thermal gradient normal to the surface of the specimen, and an error of about +60 percent due to translucent specimens. Use of a graphite post to replace the shallow cavity reduced the error by about one half, and use of a deep cavity with a graphite bottom reduced the error to about +10 percent.

2. Preparation of Specimens. Specimens of alumina, thoria, magnesia and zirconia were prepared for measurement of total normal emittance by the center post method and by the deep cavity method. Normal spectral emittance data at temperatures up to 1600°K have been obtained on these materials by the rotating cylinder method.

Specimens of boron nitride were prepared for measurement by the shallow cavity method. This material is essentially opaque over the spectral range where most of the thermal radiation is emitted at high temperatures, and hence should not have any appreciable translucency error.

The total normal emittance of all of these specimens will be measured at temperatures up to the highest that the specimens or equipment will withstand.

Graphite susceptors were fabricated for use with the center post and deep cavity methods. The fabrication necessitated very precise machining of graphite, particularly for the susceptors for the center post method. If the method is to work successfully, it is necessary that good thermal contact be maintained between the susceptor with a 0.040-in. center post and the hollow cylindrical specimen which surrounds it.

3. Repairs to Equipment. A relay timing device on the radio frequency generator burned out, and had to be replaced. As a result, the equipment was inoperative for several weeks.

After the radio frequency generator was repaired, the entire equipment was thoroughly checked and serviced. The detector-amplifier system was rechecked for linearity of response and adjusted for peak performance. All optical elements were cleaned and realigned, to give a clearly focused image of uniform intensity.

4. Error Analysis. The analysis of the scattering error presented in the report for the period November 1, 1964 through January 31, 1965, was reviewed in the light of the planned measurements with the graphite susceptors by the center post and deep cavity methods. Because of the fourfold increasein area of the reference surface (from about 0.020 to about 0.040 in. diameter) and the higher emittance of the graphite susceptor as compared to the platinum susceptor used in previous measurements, it was thought possible that there might be significant amounts of flux that originated from the reference surface or susceptor and were scattered so that they contributed to the specimen reading. Experiments are planned to measure the contributions of scattered flux to both the specimen and reference measurements.

5. Computation of Thermal Gradients.

a. Interreflection Algebra. Various schemes have been used in the past for calculating the heat transfer within a diffusely reflecting and emitting cavity. All of these methods somehow reduce to the solution of N linear equations in N unknowns--or its equivalent--the inversion of an N x N matrix. The procedures involved in radiant transfer calculations are well known; however, the clarity of the concepts involved may perhaps be enhanced when they are expressed in terms of transformations on an N-dimensional vector space.

There are three basic types of relations that must be expressed. They are given in the following equations.

$$B(\underset{\sim}{x}) = \rho(\underset{\sim}{x})\ H(\underset{\sim}{x}) \tag{1}$$

$$Q_\alpha = \int_c H(\underset{\sim}{x})\ \alpha(\underset{\sim}{x})\ dA(\underset{\sim}{x}) \tag{2}$$

$$H(\underset{\sim}{x}) = \int_c B(\underset{\sim}{x})\ K(\underset{\sim}{x}_o, \underset{\sim}{x})\, dA(\underset{\sim}{x}_o) \tag{3}$$

where $B(\underset{\sim}{x})$ is the flux per unit area leaving an element of area $dA(\underset{\sim}{x})$ located at $\underset{\sim}{x}$, $\rho(\underset{\sim}{x})$ is the reflectance of the surface at $\underset{\sim}{x}$, $H(\underset{\sim}{x})$ is the flux per unit area incident on the surface at $\underset{\sim}{x}$, Q_α is the amount of flux absorbed in a cavity when the incident flux per unit area $H(\underset{\sim}{x})$ falls on each point $\underset{\sim}{x}$ on the cavity surface, $\alpha(\underset{\sim}{x})$ is the absorptance of the cavity surface at the point $\underset{\sim}{x}$, and $\int_c$ indicates the integral over the cavity. $K(\underset{\sim}{x}_o, \underset{\sim}{x})$ is the diffuse angle factor or "geometric factor" between an element of area $dA(\underset{\sim}{x}_o)$ from which flux is diffusely radiating and the element of area $dA(\underset{\sim}{x})$ which receives the flux.

Each one of the functions $H(\underset{\sim}{x})$, $\rho(\underset{\sim}{x})$, $B(\underset{\sim}{x})$, and $\alpha(\underset{\sim}{x})$ can be thought of as vectors in an infinite dimensional vector space, and each can be expressed in terms of some complete set of basis functions (basis vectors) in that space. Since this functional vector space has an infinite number of dimensions, an infinite number of basis vectors are required to span the space. Thus, a given function may require an infinite number of component basis functions for its expression. Obviously no one can do a practical calculation with an infinite number of components for each vector, so it has been customary to reduce the number of dimensions of the space to some finite number N when any practical calculation is done. This is a familiar procedure in physics and engineering. For example, if one wants to express a complex periodic function in terms of its Fourier components, one, in general, must use an infinite number of components. If, however, one has some practical calculation to do, it is necessary to stop with some finite number of components.

An interreflection calculation is very similar. Strictly speaking, equations (1), (2), and (3) are statements about each one of the infinite number of mathematical points on a cavity surface; but, to get practical results, it is customary to express the infinitely fine-grained information in the function $B(\underset{\sim}{x})$ in terms of a coarse-grained N dimensional vector $\underset{\sim}{B}$, and instead of considering the infinitesimal surface element $dA(\underset{\sim}{x})$, we consider a number of finite surface areas ΔA_i arranged in vector form $\underset{\sim}{\Delta A}$. It is the same with $H(\underset{\sim}{x})$, $\rho(\underset{\sim}{x})$, $\alpha(\underset{\sim}{x})$, or any function of $\underset{\sim}{x}$.

$$H(\underset{\sim}{x}) \rightarrow \begin{bmatrix} H_1 \\ H_2 \\ \cdot \\ \cdot \\ \cdot \\ H_N \end{bmatrix} = \underset{\sim}{H} \qquad B(\underset{\sim}{x}) \rightarrow \begin{bmatrix} B_1 \\ B_2 \\ \cdot \\ \cdot \\ \cdot \\ B_N \end{bmatrix} = \underset{\sim}{B} \qquad dA(\underset{\sim}{x}) \rightarrow \begin{bmatrix} \Delta A_1 \\ \Delta A_2 \\ \cdot \\ \cdot \\ \cdot \\ \Delta A_N \end{bmatrix} = \underset{\sim}{\Delta A} \tag{4}$$

In the following we will denote the N-dimensional column vector corresponding to any function $w(\underset{\sim}{x})$ by the vector symbol $\underset{\sim}{w}$. The component w_i is an average value of the function $w(\underset{\sim}{x})$ on the area ΔA_i; mathematically it is just

$$w_i = \int_{\Delta A_i} \frac{w(\underset{\sim}{x})\, dA(\underset{\sim}{x})}{\Delta A_i} \tag{5}$$

With these kinds of vectors in the vector space, it is desired that the theory be a complete analogue of the functional theory. Thus equations (1), (2), and (3) must be expressible in a vector form. In order to do this, it will be very helpful if we first consider the set of basis vectors that will be used.

The most convenient set of N basis vectors $\left\{ \mathbb{1}_i \right\}_{i=1}^{i=N}$ is the one which gives us $B = \Sigma_i B_i \mathbb{1}_i$. Then the basis vectors have the ordinary representation

$$\mathbb{1}_1 = \begin{bmatrix} 1 \\ 0 \\ \vdots \\ 0 \end{bmatrix} \quad \mathbb{1}_2 = \begin{bmatrix} 0 \\ 1 \\ \vdots \\ 0 \end{bmatrix} \quad \mathbb{1}_N = \begin{bmatrix} 0 \\ 0 \\ \vdots \\ 1 \end{bmatrix} \tag{6}$$

and the vector $\underset{\sim}{B}$ has (for example) the following form.

$$\underset{\sim}{B} = \begin{bmatrix} B_1 \\ B_2 \\ \vdots \\ B_N \end{bmatrix} \tag{7}$$

The vector space analogy of Equation (1) is $\underset{\sim}{B} = \underset{\sim}{\rho}\, \underset{\sim}{H}$ (8)

$$\Sigma_i B_i \mathbb{1}_i = \Sigma_i (\rho_i \mathbb{1}_i) \Sigma_j (H_j \mathbb{1}_j) = \Sigma_{i,j} \rho_i H_j \mathbb{1}_i \mathbb{1}_j \tag{9}$$

In the above equations a vector valued multiplication operates in the vector space. This type of vector multiplication must be commutative, distributive and associative, because it must be the analog of the ordinary multiplication of functions. In addition the multiplication operation must be linear in the sense that if a and b are any real numbers and if $\underset{\sim}{u}$, $\underset{\sim}{v}$, and $\underset{\sim}{w}$ are any vectors,

then $\underset{\sim}{u}\ (a\underset{\sim}{v} + b\underset{\sim}{w}) = a\ (\underset{\sim}{u}\ \underset{\sim}{v}) + b\ (\underset{\sim}{uw})$ (10)

and $(a\underset{\sim}{v} + b\underset{\sim}{w})\ \underset{\sim}{u} = a\ (\underset{\sim}{vu}) + b\ (\underset{\sim}{wu})$ (11)

A vector space having a vector valued multiplication operation which is linear, associative, and distributive is known as a <u>linear algebra.</u>

A linear multiplication operation in a vector space can be specified by giving the rule for the multiplication of the set of basis vectors amongst each other; that is

$$\underset{\sim}{xy} = \sum_{i,j} x_i \underset{\sim}{\eta}_i \, y_j \underset{\sim}{\eta}_j = \sum_{i,j} x_i \, y_i \underset{\sim}{\eta}_i \underset{\sim}{\eta}_j \tag{12}$$

and if all the vectors $\underset{\sim}{\eta}_i \underset{\sim}{\eta}_j$ are known then the multiplication operation is completely specified. In the case which we have under discussion the multiplication table for the basis vectors is quite simple (Table 1). The rule is

$$\underset{\sim}{\eta}_i \; \underset{\sim}{\eta}_j = \delta_{ij} \underset{\sim}{\eta}_i \tag{13}$$

where δ_{ij} is the Kronecker delta

$$\delta_{ij} = 1 \quad \text{iff } i = j$$
$$\delta_{ij} = 0 \quad \text{iff } i \neq j. \tag{14}$$

Table 1.

	0	$\underset{\sim}{\eta}_1$	$\underset{\sim}{\eta}_2$	$\underset{\sim}{\eta}_3$ . . .
0	0	0	0	0
$\underset{\sim}{\eta}_1$	0	$\underset{\sim}{\eta}_1$	0	0
$\underset{\sim}{\eta}_2$	0	0	$\underset{\sim}{\eta}_2$	0
$\underset{\sim}{\eta}_3$	0	0	0	$\underset{\sim}{\eta}_3$
⋮				

Also there exists a vector $\underset{\sim}{1}$ analgous to the scalar 1 such that for any vector $\underset{\sim}{w}$

$$\underset{\sim}{1} \; \underset{\sim}{w} = \underset{\sim}{w} \; \underset{\sim}{1} = \underset{\sim}{w} \tag{15}$$

Written out longhand the vector $\underset{\sim}{1}$ is

$$\begin{pmatrix} 1 \\ 1 \\ 1 \\ \cdot \\ \cdot \\ 1 \end{pmatrix} \tag{16}$$

For every vector $\underset{\sim}{w}$ such that none of the components of $\underset{\sim}{w}$ is equal to zero, there exists a vector $\underset{\sim}{w}^{-1}$ such that $\underset{\sim}{w} \; \underset{\sim}{w}^{-1} = \underset{\sim}{1}$. The vector $\underset{\sim}{w}^{-1}$ can be easily constructed when $\underset{\sim}{w}$ is known. If $\underset{\sim}{w} = \sum_i w_i \underset{\sim}{\eta}_i$, then $\underset{\sim}{w}^{-1} = \sum_i (1/w_i) \underset{\sim}{\eta}_i$. It is easy to see that if any w_i is equal to zero, no finite inverse vector for $\underset{\sim}{w}$ exists, since the magnitude of one of the components of $\underset{\sim}{w}^{-1}$ would be 1/0.

One of the more important theorems that one can prove about a linear algebra is that for each N-dimensional linear algebra there exists an isomorphic set of N x N linear transformations (matrices) such that the operations of vector addition and multiplication and also multiplication by a scalar (real number) are preserved under the isomorphism[1/]. (An isomorphism is a one-to-one correspondence between two sets such that the structure of certain operations in those sets is preserved).

It is not difficult at all to find the set of matrices which is isomorphic to the set of vectors under consideration.

The vector equation (in long form) is:

$$\begin{bmatrix} \rho_1 H_1 \\ \rho_2 H_2 \\ \vdots \\ \rho_N H_N \end{bmatrix} = \begin{bmatrix} \rho_1 \\ \rho_2 \\ \vdots \\ \rho_N \end{bmatrix} \begin{bmatrix} H_1 \\ H_2 \\ \vdots \\ H_N \end{bmatrix} \tag{17}$$

This can be represented equally well by a product of diagonal matrices.

$$\begin{bmatrix} \rho_1 H_1 & 0 & \cdots & 0 \\ 0 & \rho_2 H_2 & & \\ \vdots & & \ddots & 0 \\ 0 & & 0 & \rho_N H_N \end{bmatrix} = \begin{bmatrix} \rho_1 & 0 & \cdots & 0 \\ 0 & \rho_2 & & \\ \vdots & & \ddots & 0 \\ 0 & \cdots & 0 & \rho_N \end{bmatrix} \begin{bmatrix} H_1 & 0 & \cdots & 0 \\ 0 & H_2 & & \vdots \\ \vdots & & \ddots & \vdots \\ 0 & \cdots & & H_N \end{bmatrix} \tag{18}$$

It is easy to see that the matrix multiplication in equation (18) does essentially the same thing with the i^{th} diagonal elements of the matrices as the vector multiplication in equation (17) does with the i^{th} components of the vectors. One can see intuitively that an isomorphism exists and the proof of this is quite easy also.

It is easy to show that vector addition and scalar multiplication are preserved under this isomorphism. We can denote the isomorphism by τ and its inverse τ^{-1} such that

$$\tau \begin{bmatrix} w_1 \\ w_2 \\ \\ w_N \end{bmatrix} = \begin{bmatrix} w_1 & 0 & 0 \\ 0 & w_2 & \\ & & \ddots \ 0 \\ 0 & & w_N \end{bmatrix} \tag{19}$$

[1/] G. Birkhoff and S. MacLane, A survey of Modern Algebra, p. 216

and

$$\tau^{-1}\begin{pmatrix} w_1 & 0 & \cdots & 0 \\ 0 & w_2 & & \vdots \\ \vdots & & \ddots & \\ 0 & \cdots & & w_N \end{pmatrix} = \begin{pmatrix} w_1 \\ w_2 \\ \\ w_N \end{pmatrix} \tag{20}$$

If we denote vector by a vector symbol $\underset{\sim}{w}$, then we can denote the diagonal matrix which corresponds to $\underset{\sim}{w}$ by $\tau(\underset{\sim}{w})$; however, the notation would be somewhat simplified if one simply denoted the operator by removing the vector symbol,for example

$$\tau(\underset{\sim}{w}) = w. \tag{21}$$

It is a useful property of these diagonal matrices that the operation of one, say $\underset{\sim}{w}$, by ordinary matrix multiplication on a vector $\underset{\sim}{v}$ gives the same result as the multiplication of the original vector $\underset{\sim}{w}$ on the vector $\underset{\sim}{v}$, i.e. for any vectors $\underset{\sim}{v}$, $\underset{\sim}{w}$

$$\underset{\sim}{wv} = w\underset{\sim}{v} = \tau(\underset{\sim}{w})\underset{\sim}{v} \tag{22}$$

The next operation for which we wish to find an analogue is shown in equation (2). In this equation two functions $H(\underset{\sim}{x})$ and $\rho(\underset{\sim}{x})$,(or three functions if we consider $dA(\underset{\sim}{x})$ as a function) are operated on so as to give a scalar (single number) result Q_α.

In vector space language this is denoted by $[\underset{\sim}{A}, \underset{\sim}{B}, \underset{\sim}{C}]$.

$$Q_\alpha = [\underset{\sim}{\alpha}, \underset{\sim}{H}, \underset{\sim}{\Delta A}] \tag{23}$$

This is called a trilinear form because it maps three vectors, $\underset{\sim}{\alpha}$, $\underset{\sim}{H}$, and $\underset{\sim}{\Delta A}$, into a scalar Q_α in a linear fashion, i.e., linear in the sense that for any scalars γ, λ, and vectors $\underset{\sim}{w}$, $\underset{\sim}{x}$, $\underset{\sim}{y}$, and $\underset{\sim}{z}$,

$$[\gamma\underset{\sim}{w} + \lambda\underset{\sim}{x}, \underset{\sim}{y}, \underset{\sim}{z}] = \gamma[\underset{\sim}{w}, \underset{\sim}{y}, \underset{\sim}{z}] + \lambda[\underset{\sim}{x}, \underset{\sim}{y}, \underset{\sim}{z}]$$

$$[\underset{\sim}{w}, \gamma\underset{\sim}{x} + \lambda\underset{\sim}{y}, \underset{\sim}{z}] = \gamma[\underset{\sim}{w}, \underset{\sim}{x}, \underset{\sim}{z}] + \lambda[\underset{\sim}{w}, \underset{\sim}{y}, \underset{\sim}{z}] \tag{24}$$

$$[\underset{\sim}{w}, \underset{\sim}{x}, \gamma\underset{\sim}{y} + \lambda\underset{\sim}{z}] = \gamma[\underset{\sim}{w}, \underset{\sim}{x}, \underset{\sim}{y}] + \lambda[\underset{\sim}{w}, \underset{\sim}{x}, \underset{\sim}{z}]$$

In addition the trilinear form that is considered here has the special property that it is equivalent to a bilinear form on two vectors, one of which is the vector product of the other two.

$$Q_\alpha = [\underset{\sim}{\alpha}, \underset{\sim}{H}\underset{\sim}{\Delta A}] \tag{25}$$

Also it can be considered as a linear functional of the one triple product vector

$$Q_\alpha = [\underset{\sim}{\alpha}\underset{\sim}{H}\underset{\sim}{\Delta A}] \tag{26}$$

This final operation--the linear functional shown in equation (26)--is perhaps the most useful and most easily understood operation. Q_α is just the sum of all of the components of the vector $(\underset{\sim}{\alpha H \Delta A})$.

The set of all possible linear functionals on a vector space constitutes a vector space, which is closely related to the original vector space. The vector space of linear functionals is known as the dual space of the original vector space, and each vector in the original vector space has a conjugate vector (or linear functional) in the dual space. In quantum mechanics this is symbolized by the famous bra or ket notation of Dirac. A bra is the symbol $<|$, and a ket is the symbol $|>$. A ket stands for a vector; and if the vector has a name, say α, then the ket is written as $|\alpha>$. Similarly a bra stands for a linear functional or a vector in the dual space to the original vector space. The vector isomorphic to the ket $|\alpha>$ is the bra $<\alpha|$. Since the scalar field onto which these linear functionals map the vectors is the field of real numbers, we do not have to worry about the complications that ordinarily arise in quantum mechanics because a complex scalar field is used. In order to construct the basis of the dual space, one constructs the set of linear functionals $\left\{<\gamma_i|\right\}_{i=1}^{i=N}$ which are such that any one of these operating on its conjugate basis vector $|\eta_i>$ gives the value 1 and operating on any other basis vector gives the value 0. Thus the set of basis vectors $\left\{<\gamma_i|\right\}$ in the dual space is constructed such that

$$<\gamma_i|\eta_j> = \delta_{ij} \tag{27}$$

where δ_{ij} is the Kronecker delta function. In terms of these operators then we have

$$Q_\alpha = <1|\ \alpha H \Delta A> = \left(\sum_i <\gamma_i|\right)\left(\sum_j \alpha_j\ H_j\ \Delta A_j\ |\eta_j>\right) \tag{28}$$

$$= \sum_{i,j} \alpha_i H_i \Delta A_j <\gamma_i|\eta_j> = \sum_{ij} \alpha_i\ H_i\ \Delta A_j \delta_{ij} = \sum_j \alpha_j\ H_j\ \Delta A_j$$

In terms of the operators corresponding to the vectors, this equation is

$$Q_\alpha = <1|\alpha H \Delta A|1> \tag{29}$$

since α, H and dA are symmetric (Hermetian) operators

$$Q_\alpha = <\alpha|\ H\ |\ \Delta A> \tag{30}$$

A second way of expressing equation (2) is completely in terms of the operators α, H and dA and the trace operation.

$$Q_\alpha = \text{trace } (\alpha H \Delta A) \tag{31}$$

where the trace of a matrix is the sum of its diagonal terms, for example

$$\text{trace } M = \text{trace} \begin{pmatrix} M_{11} & M_{12} & M_{13} \\ M_{21} & M_{22} & M_{23} \\ M_{31} & M_{32} & M_{33} \end{pmatrix} = M_{11} + M_{22} + M_{33} \tag{32}$$

thus

$$Q_\alpha = \text{trace} \begin{pmatrix} \alpha_1 H_1 \Delta A_1 & 0 & 0 \cdots 0 \\ 0 & \alpha_2 H_2 \Delta A_2 & \vdots \\ \vdots & 0 & \ddots \; 0 \\ 0 & \cdots & 0 \; \alpha_N H_N \Delta A_N \end{pmatrix} = \sum_{i=1}^{N} \alpha_i H_i \Delta A_i \tag{33}$$

Finally we want to express equation (3) in vector form. This is not difficult since the operator $\int_c K(\underset{\sim}{x}_0,\underset{\sim}{x}) dA(\underset{\sim}{x}_0)$ acting on the function $B(\underset{\sim}{x}_0)$ is a linear transformation; that is, it obeys the following relation:

$$\int_c (\alpha B_1(\underset{\sim}{x}_0) + \beta B_2(\underset{\sim}{x}_0)) K(\underset{\sim}{x}_0,\underset{\sim}{x}) \, dA(\underset{\sim}{x}_0) = \alpha \int_c B_1(\underset{\sim}{x}_0) K(\underset{\sim}{x}_0,\underset{\sim}{x}) \, dA(\underset{\sim}{x}_0) + \beta \int_c B_2(\underset{\sim}{x}_0) K(\underset{\sim}{x}_0,\underset{\sim}{x}) \, dA(\underset{\sim}{x}_0) \tag{34}$$

For any numbers α, β, and functions B_1, B_2.

The function $B(\underset{\sim}{x})$ is of course represented by the vector $\underset{\sim}{B}$ and the operation $\int_c B(\underset{\sim}{x}_0) K(\underset{\sim}{x}_0,\underset{\sim}{x}) \, dA(\underset{\sim}{x}_0)$ is represented by performing a linear transformation on $\underset{\sim}{B}$. A theorem states that any linear transformation on a vector in an N-dimensional vector space may be represented by the multiplication of the vector by an N x N matrix. One method of calculating the elements of this matrix is to consider the case in which each area ΔA_j is uniformly radiating a constant diffuse flux per unit area B_j. Then the cavity surface integral is broken into N integrals over the sub areas $\{\Delta A_j\}_{j=1}^{j=N}$ of the cavity. Equation (3) becomes:

$$H(\underset{\sim}{x}) = \sum_{j=1}^{N} \int_{\Delta A_j} B_j K(\underset{\sim}{x}_0,\underset{\sim}{x}) \, dA(\underset{\sim}{x}_0) = \sum_{j=1}^{N} B_j \int_{\Delta A_j} K(\underset{\sim}{x}_0,\underset{\sim}{x}) \, dA(\underset{\sim}{x}_0) \tag{35}$$

If we evaluate the average flux incident on each ΔA_i we have

$$H_i = \frac{\int_{\Delta A_i} H(\underset{\sim}{x})\, dA(\underset{\sim}{x})}{\Delta A_i} \tag{36}$$

This gives us

$$H_i = \sum_{j=i}^{N} B_j \frac{\int_{\Delta A_i}\int_{\Delta A_j} K(\underset{\sim}{x}_o, \underset{\sim}{x})\, dA(\underset{\sim}{x}_o)\, dA(\underset{\sim}{x})}{\Delta A_i} \tag{37}$$

If we define the matrix K by

$$K = (K_{ij}) = \left(\frac{\int_{\Delta A_i}\int_{\Delta A_j} K(\underset{\sim}{x}_o, \underset{\sim}{x})\, dA(\underset{\sim}{x}_o)\, dA(\underset{\sim}{x})}{\Delta A_i \Delta A_j} \right) \tag{38}$$

then we have, from equation (37),

$$\underset{\sim}{H} = K(\Delta A\, \underset{\sim}{B}) \tag{39}$$

and since $K(\underset{\sim}{x}_o, \underset{\sim}{x}) = K(\underset{\sim}{x}, \underset{\sim}{x}_o)$, we have $K_{ij} = K_{ji}$.

There is another useful way to look at this problem. Under the above conditions the total flux leaving the j-th sub area is $\Delta A_j B_j$ and the amount of flux reaching the i-th area from the j-th area is just $\Delta A_i K_{ij} \Delta A_j B_j$; so the fraction F_{j-i} of the flux leaving ΔA_j and arriving at ΔA_i is given by

$$F_{j-i} = \Delta A_i K_{ij} \tag{40}$$

$$\text{and} \quad F_{i-j} = \Delta A_j K_{ij} = \frac{\Delta A_j}{\Delta A_i} F_{j-i}$$

In matrix form this is

$$F = K\Delta A \tag{41}$$

And equation (3) has the analogue

$$\underset{\sim}{H} = F\underset{\sim}{B} \tag{42}$$

The net local heat loss q_i at each ΔA_i on the cavity surface must be known for the thermal gradient calculation. One has the following equations:

$$\underset{\sim}{B} = \epsilon\sigma \underset{\sim}{T}^4 + \rho\underset{\sim}{H} \tag{43}$$

$$\underset{\sim}{q} = \epsilon\sigma \underset{\sim}{T}^4 - \epsilon\underset{\sim}{H} \tag{44}$$

$$\underset{\sim}{H} = K\Delta A\, \underset{\sim}{B} \tag{45}$$

Combining (43) with (45), we obtain

$$\underset{\sim}{B} = \epsilon\sigma\underset{\sim}{T}^4 + \rho K\triangle A\underset{\sim}{B} \; . \tag{46}$$

This gives

$$(1 - \rho K\triangle A)\underset{\sim}{B} = \epsilon\sigma\underset{\sim}{T}^4 \tag{47}$$

Physical reasoning tells us that the inverse matrix $(1 - \rho K\triangle A)^{-1}$ must exist, so we can write

$$\underset{\sim}{B} = (1 - \rho K\triangle A)^{-1}\epsilon\sigma\underset{\sim}{T}^4 \tag{48}$$

The above equation is the solution for $\underset{\sim}{B}$ in terms of $\underset{\sim}{T}^4$ and geometry. To complete the derivation, we need an expression for $\underset{\sim}{q}$ in terms of $\underset{\sim}{B}$ and $\underset{\sim}{T}^4$. Equation (43) gives us

$$\underset{\sim}{H} = \rho^{-1}(\underset{\sim}{B} - \epsilon\sigma\underset{\sim}{T}^4) \tag{49}$$

Substituting this result into equation (44) one obtains

$$\underset{\sim}{q} = \epsilon\sigma\underset{\sim}{T}^4 - \epsilon\rho^{-1}(\underset{\sim}{B} - \epsilon\sigma\underset{\sim}{T}^4) \tag{50}$$

Taking $\underset{\sim}{B}$ from equation (48), one obtains

$$\underset{\sim}{q} = \epsilon\sigma\underset{\sim}{T}^4 - \epsilon\rho^{-1}((1-\rho K\triangle A)^{-1}\epsilon\sigma\underset{\sim}{T}^4 - \epsilon\sigma\underset{\sim}{T}^4) = [1-\epsilon\rho^{-1}((1-\rho K\triangle A)^{-1}-1)]\epsilon\sigma\underset{\sim}{T}^4$$
$$= \mathfrak{F}\,\epsilon\sigma\underset{\sim}{T}^4 \tag{51}$$

where

$$\mathfrak{F} = [1+\epsilon\rho^{-1}(1-(1-\rho K\triangle A)^{-1})] \tag{52}$$

Thus we can obtain the complete transfer solution matrix $\mathfrak{F}$ from a knowledge of K and ϵ. Equivalent prescriptions for obtaining this matrix have been given numerous times in the literature. In the present development the roles of matrix multiplication and inversion have been emphasized and the isomorphism between the vector $\underset{\sim}{\mathfrak{E}}$ and the matrix operation ϵ(or $\tau(\underset{\sim}{\mathfrak{E}})$) were described. This may help to clarify the mathematical situation because any equation involving expressions like those in equations (1), (2) or (3) can be written down quickly in terms of vectors, linear transformations, linear functionals, or traces.

b. Angle Factors in a Cylindrical Cavity. The angle factors between various areas ($\triangle A_i$) on the surface of a cylindrical cavity are relatively easy to evaluate. An expression for the fraction F_{i-j} of the diffuse flux leaving a given area, $\triangle A_i$, which falls directly on any other area, $\triangle A_j$, is needed. The cavity base is divided into a series of annular rings and the wall is divided into a series of cylindrical rings (Figure 1).

The angle factor between any two cylindrical rings of equal width, h, can be expressed as

$$F_3(d,R,h) = F_2(d-5h,R,h) - F_2(d+5h,R,h) \qquad (53)$$

where d is the distance between the centers of the two rings, and R is the radius of the cylinder.

In the above equation, the function $F_2(d,R,h)$ is given by

$$F_2(d,R,h) = \frac{R}{2h} F_1(d,R,h) \qquad (54)$$

where

$$F_1(d,R,h) = F_o(d-5h,R) - F_o(d+5h,R) \qquad (55)$$

and

$$F_o(d,R) = \left\{d^2+2R^2-\left[(d^2+2R^2)^2 - 4R^4\right]^{1/2}\right\}(2R^2)^{-1} \qquad (56)$$

The derivation of the above series of functional relationships proceeds as follows. $F_o(d,R)$ gives the fraction of the diffuse flux, leaving a circular disc of radius R, which is incident on a parallel circular disc of equal radius when the two discs are a distance d apart on the same axis (Figure 2). This equation is given by Walsh[2/] for discs of unequal radii.

$F_1(d,R,h)$ is the fraction of the flux leaving disc 1 of radius R and reaching cylindrical ring 2 of radius R and width h whose center is located a distance d above the center of disc 1 (Figure 3). This fraction can be considered to be the difference between the fraction reaching disc 3 and that reaching disc 4 (Figure 3), and this is expressed in equation (55). The fraction $F_2(d,R,h)$ of the flux leaving ring 2 and falling directly on disc 1 (in Figure 3) is easily calculated from equation (40). Finally, the fraction of the flux leaving cylindrical ring 1 and reaching cylindrical ring 2 is given by $F_3(d,R,h)$ in equation (53) above; $F_3(d,R,H)$ is expressed as the difference between the fraction leaving ring 1 and arriving at disc 3 and the fraction leaving ring 1 and arriving at disc 4 (Figure 4).

2/ J. W. T. Walsh, Proc. Phys. Soc. (London) 32, 59 (1920).

Similar reasoning gives the following series of functional relationships for the fraction $F_3'(R,h,d,r)$ of the flux leaving an annular ring 1 of width h and mean radius r on the base of a cylindrical cavity and falling incident on cylindrical ring 2 of width h located a mean distance d above the cavity base (Figure 5).

$$F_3'(R,h,d,r,h) = F_2'(R,d-.5h,r,h) - F_2'(R,d+.5h,r,h) \qquad (57)$$

$$F_2'(R,h,r,h) = \frac{R^2 F_1'(R,d,r,h)}{((r+.5h)^2-(r-.5h)^2)} \qquad (58)$$

$$F_1'(R,d,r,h) = F_o'(R,r+.5h,d) - F_o'(R,-.5h,d) \qquad (59)$$

$$F_o'(d,R,r) = \left\{d^2+R^2+r^2-[(d^2+r^2+R^2)^2-4R^2r^2]^{1/2}\right\}(2R^2)^{-1} \qquad (60)$$

The fraction $F_4'(R,h,d,r,h)$ of the flux leaving cylindrical ring 2 of width h located a mean distance d above the base of the cylindrical cavity and incident on an annular ring of width h and mean radius r on the cavity base is given by

$$F_4'(R,h,d,r,h) = \frac{((r+.5h)^2-(r-.5h)^2)}{2Rh} F_3'(R,h,d,r,h) \qquad (61)$$

These functional relationships have been incorporated into a subroutine of the computer program that will calculate the temperature distribution in the cylindrical specimen. This subroutine is currently under development.

c. Radiant Heat Transfer. The computer code mentioned in the previous quarterly report was developed further and some results were obtained. The code is not completely satisfactory because it does not yet yield good agreement with hand-calculated results. The geometry of the calculation is that of Figure 6. The temperatures of volumes 5 through 10 are all fixed at a temperature of 2000°K and the temperatures of volumes 1 through 4 are permitted to come to an equilibrium temperature in these surroundings. The temperatures of volumes 1 through 4 are determined by the condition that the total heat flux into each volume equals the total heat flux leaving that volume. This condition gives us four equations in four unknowns.

$$0 = s_i = \frac{A_i \epsilon^2 \sigma}{\rho} \sum_{j=i}^{4} P_{ij} T_j^4 + \sum_{j=i}^{4} \frac{kA_{ij}}{h_{ij}} (T_j - T_i) \quad (i=1,\ldots,4) \qquad (62)$$

Where s_i is the difference between the heat flowing into the i-th volume element and that flowing out of it, ϵ is the emittance of the material, ρ is the reflectance of the material, σ is the Stefan-Boltzmann constant,

T_i is the temperature of the i-th volume, k is the conductivity of the material, A_i is the exposed surface area of the i-th volume element, h_{ij} is the distance between the center of the i-th volume to that of the j-th volume. P_{ij} is the (i,j)th element of a matrix P which is similar to the $\tilde{S}$ matrix discussed elsewhere in this report.

The method of solving these equations is a relaxation procedure. The first step is to guess a set of T_i's; then the s_i's are evaluated. The s_i's describe the imbalance in the amount of heat flux entering or leaving a volume, and they are called residues. A positive s_i means that too much heat is flowing into the i-th subvolume and that the temperature of this subvolume must be too low for its environment. Conversely a negative s_i implies too great a heat loss and hence too high a temperature for the i-th volume. The volume having the largest $|s_i|$ is the one farthest from thermal equilibrium. The temperature of this volume is then changed in uniform steps until the magnitude of the residue is made as small as possible. Then all of the residues are recalculated using the new T_i for the i-th volume and the old T_i's for the others. The volume having the largest residue for this new set of temperatures is again singled out and the procedure is repeated. After this process is repeated many times, the magnitude of each residue reaches some very small value. At this point changing any of the temperatures by the uniform step used will only increase the magnitude of the thermal imbalance in the system. It is highly probable that when this condition is achieved, each of the temperatures is within a few uniform steps of the value it would have when they are all picked to satisfy equation (1) exactly.

This procedure has been used both in a hand and computer calculation of the heat transfer described in equation (1). The results of the two calculations are shown in Table 2.

Table 2

	Hand Code	Computer
T_1	1958°K	1957°K
T_2	1981°K	1980°K
T_3	1993°K	1992°K
T_4	1987°K	1979°K

The agreement is good for T_1, T_2 and T_3. However the variation in T_4 is appreciable. Further checks are being made on both the hand calculation and on the computer code to try to achieve better agreement.

d. Conductive Heat Transfer in the Cylinder. The conductive heat transfer within the cylindrical specimen must be known in order to determine the temperature distribution at the specimen's surface. The equation of steady state heat transfer within the specimen is

$$\frac{\partial^2 T}{\partial r^2} + \frac{1}{r}\frac{\partial T}{\partial r} + \frac{\partial^2 T}{\partial z^2} = 0 \qquad (63)$$

where T is the temperature. The solution of equation (63) is determined by the boundary conditions at the specimen's surfaces. The solution will be calculated by a code now being developed which uses the finite difference method for solving equation (63). This code will be in such a form that it will be able to handle all three cases of interest, the shallow cavity, the deep cavity, and the graphite post configurations. In order to perform this finite difference calculation, a series of node points must be located throughout the specimen, and the equation for the temperature at each node must be written in terms of the temperatures at the neighboring nodes. It is natural to divide the specimen into different regions such that the same equation holds for all of the nodes in a given region. The distribution of the nodes throughout the specimen, the division of the specimen into regions, and the equations corresponding to each region will be described in the following.

The nodes are distributed throughout the specimen and cavity in a square lattice spaced a distance h apart from each other in the z and r directions (Figure 7). Each node is labelled with a pair of indices (i, j) such that $1 \leq i \leq i_{max}$ as $0 \leq r \leq c$, and $1 \leq j \leq j_{max}$ as $0 \leq z \leq b$. The possibility that the radius, c, and length, b, of the specimen may not be evenly divisible by the distance h between nodes is taken into account by letting the distances between the nodes on the exterior surface of the specimen and those immediately beside or above them inside the specimen become a fraction α_1 or α_2 of the usual distance h.

After the nodes are distributed in the specimen, the specimen must be divided into regions which have the same nodal equations. There are eleven such regions in a shallow cavity specimen. In order to describe these regions mathematically, we need to make the following definitions:

i_{cav} = The i-index of the column of nodes on the cavity wall surface

j_{cav} = The j-index of the row of nodes on the cavity base

i_{max} = The i-index of the column of nodes on the specimen wall surface

j_{max} = The j-index of the column of nodes on the specimen base surface

The regions are described by the following:

A1: $i < i_{max}$ and $j = j_{max}$

A2: $1 < i < i_{max}-1$ and $j = j_{max}-1$

A3: $i = 1$ and $j_{cav} < j < j_{max}-2$

A4: $i \leq i_{cav}$ and $j = j_{cav}$ or $i = i_{cav}$ and $j \leq j_{cav}$

A5: $i<i_{cav}$ and $j<j_{cav}$

A6: $i_{cav}<i<i_{max}$ and $j = 1$

A7: $i = i_{max}$ and $1\leq j\leq j_{max}$

A8: $i = i_{max}-1$ and $1<j<j_{max}-2$

A9: $i_{cav}<i\leq i_{max}-1$ and $1<j<j_{max}-1$

or $1<i\leq i_{cav}$ and $j_{cav}<j<j_{max}-1$

A10: $i = i_{max}-1$ and $j = j_{max}-1$

A11: $i = 1$ and $j = j_{max}-1$

The nodal equations that hold in these regions are as follows:

A1: No equation--fixed temperatures assumed.

A2: $$T_{i,j} = .5\left(\frac{\alpha_1}{\alpha_1+1}\right)\left\{T_{i-1,j}+T_{i+1,j}+\frac{h}{2R_i}\left(T_{i+1,j}-T_{i-1,j}\right)+\frac{2}{\alpha_1(\alpha_1+1)}\left(\alpha_1 T_{i,j-1}+T_{i,j+1}\right)\right\}$$

A3: $$T_{i,j} = \frac{2}{3}T_{2,j}+\frac{1}{6}\left(T_{1,j-1}+T_{1,j+1}\right)$$

A4: $$k\frac{\partial T}{\partial n} = \epsilon\sigma T^4$$

A5: No equation--fixed temperatures assumed.

A6: $$T_{i,2} = \left(-\frac{k}{h}-4\epsilon\sigma T'^{3}_{i,1}\right)^{-1}\left(3\epsilon\sigma T'^{4}_{i,1}-\frac{k}{h}T_{i,2}\right)$$

A7: No equation - fixed temperatures assumed.

A8: $$T_{i,j} = \frac{2\alpha_2 R_i}{4\alpha_2 r+4R_i-h(\alpha_2-1)}\left\{T_{i,j+1}+T_{i,j-1}+\frac{2}{\alpha_2(\alpha_2+1)}\left(\alpha_2 T_{i-1,j}+T_{i+1,j}\right)+\frac{1}{2\alpha_2 hR_i}\left(-\alpha_2 T_{i-1,j}+T_{i+1,j}\right)\right\}$$

A9: $$T_{i,j} = \frac{1}{4}\left(T_{i+1,j}+T_{i-1,j}+T_{i,j+1}+T_{i,j-1}\right) + \frac{h}{8R_i}\left[T_{i+1,j}-T_{i-1,j}\right]$$

A10: $$T_{i,j} = \frac{2\alpha_1\alpha_2 R_i}{4R_i(\alpha_1+\alpha_2)-h\alpha_1(\alpha_2-1)}\left[\frac{2}{\alpha_1(1+\alpha_1)\alpha_2(1+\alpha_2)}\left\{\alpha_1\alpha_2(1+\alpha_1)T_{i-1,j}\right.\right.$$

$$\left. + \alpha_1\alpha_2(1+\alpha_2)T_{i,j+1}+\alpha_1(\alpha_1+1)T_{i+1,j}+\alpha_2(1+\alpha_2)T_{i,j+1}\right\}$$

$$\left. + \left(2\alpha_2 hR_i\right)^{-1}\left\{-\alpha_2 T_{i-1,j}+T_{i+1,j}\right\}\right]$$

A11: $$T_{i,j} = \left(\frac{\alpha_1}{2\alpha_1+1}\right)\left(2T_{2,j}+\frac{\alpha_1 T_{i,j-1}+T_{i,j+1}}{\alpha_1(\alpha_1+1)}\right)$$

In the above equations $T^{*}_{i,j}$ designates the temperature at the node found on the previous iteration.

An iterative solution to this set of equations is found as follows. A set of trial $T_{i,j}$'s is guessed at. The trial $T_{i,j}$'s are inserted into the above equations, and a new set of $T_{i,j}$'s is calculated from the trial set. This procedure is repeated until a "self-consistent" or steady state is achiefed, i.e., the input and output $T_{i,j}$'s are nearly the same each time. When the set of $T_{i,j}$'s has reached a stationary value, it is taken as the temperature distribution within the specimen. This method of solving the conductive heat transfer problem has been used many times in the past with good results.3/

III. LASER SOURCE INTEGRATING SPHERE REFLECTOMETER

1. Background. The laser source integrating sphere reflectometer was designed to measure reflectance of specimens at high temperatures under conditions approximating normal illumination and hemispherical viewing. The sphere that was built and is described in previous reports was designed for operation in the substition mode. Tests with both first reflection only and lined shallow cavities and comparative reflectance measurements indicated that under the most favorable conditions this sphere measured reflectance to about ±0.02. The error appeared to depend upon the geometric distribution of flux reflected from specimen and standard, and was believed to be due to flux reflected from the specimen or standard reaching the detector or the area viewed by the detector on the first reflection.

3/ Daniel D. McCracken and William S. Dorn, Numerical Analysis and Fortran Programming.

2. Modifications to Sphere Design. In order to discuss the sphere design it is first necessary to describe its geometry. The sphere is made up of two hemispheres, which are joined by bolted flanges with an o-ring seal. The principal axis of the sphere is defined as the diameter normal to the plane through the joint connecting the hemispheres. The primary plane of the sphere is defined as the plane through the principal axis and the center of the entrance port, and the secondary plane of the sphere is the plane through the principal axis and normal to the primary plane.

In the original sphere the specimen port was located in the lower hemisphere and centered on the principal axis. The entrance port was centered 14° from the principal axis, and by definition was in the primary plane. There were two detector ports, one located in the lower hemisphere and centered 60° from the principal axis, and one identified as No. 3, located in the upper hemisphere and centered 45° from the principal axis in the primary plane. The two hemispheres could be rotated relative to each other, so that the detector port in the lower hemisphere could be located in the primary plane, where it was identified as No. 1, or in the secondary plane, where it was identified as No. 2.

In the modified sphere shown in Figure 8, only the No. 3 detector port was used, and the field of view of the detector was restricted to a small area of the sphere wall diametrically opposite the detector port. The single specimen port was replaced by two ports, one for the specimen and one for the comparison standard. These ports were centered in the secondary plane, 20° on either side of the principal axis. They are thus located symmetrically with respect to the entrance and detector ports.

In addition to the change in the detector ports, shields were introduced into the sphere to screen the area viewed by the detector from the specimen and comparison standard ports. Since the area viewed by the detector is located near the specimen ports, the shields are small in size and do not appreciably disturb the sphere configuration. The effect of the shields is to ensure that all of the flux reaching the detector has been reflected by the diffuse sphere lining at least twice. As a result the area viewed by the detector should be uniformly illuminated, and all problems arising from differences in the geometric distribution of flux reflected by the sample and comparison standard should be eliminated.

By operating the integrating sphere in the comparison mode, in which both the sample and comparison standard form part of the sphere wall during both measurements, the sphere corrections involving the reflectance of the sample and comparison standard are eliminated. Also, with the sphere operating in the comparison mode, it will be possible to make measurements at a number of different temperatures, and perhaps even at different wavelengths, without moving either the specimen or standard. The separation of the sample and comparison ports by 40°, about 4.8 in. on the 14-in. diameter sphere, leaves adequate space for incorporation of a specimen heater and cooling coils for the surrounding sphere wall.

3. Specimen Heater. So far, the specimen has been heated by means of resistance heating elements mounted in the specimen holder. They have been satisfactory for operation at temperatures up to about 1800°K, with heating elements that are stable in an air atmosphere. Resistance heating elements for use at higher temperatures generally require use of a non-oxidizing atmosphere surrounding the heating elements and special refractories to support the heating element and specimen. Such refractories must not only be stable at the operating temperature in the non-oxidizing atmosphere, but must also be non-reactive with the heating element and specimen. Such refractories are not readily available particularly for use at the higher temperatures. Induction heating eliminates many of these problems, and has been selected for use at the higher temperatures.

The induction heater should not disturb the sphere configuration, should be capable of heating the specimen to at least 4000°F, and should not heat the sphere wall appreciably.

Tests were made with an induction heater comprising a 3-in. diameter copper disc with a center hole just large enough to clear the susceptor, and a water cooled coil below the disc. The disc was slotted, to reduce heating and concentrate the field around the susceptor, and the first turn of the coil was soldered to the disc, to provide some cooling. A stainless steel plate with a 3-in. diameter hole was mounted above the heater, and a nickel susceptor mounted in the heater was held at about 1400°K for several minutes. Only slight heating of the stainless steel plate was observed, and this amount of heat could be easily removed by the water cooling. In the final design of the sphere, there will be a 1/2-in. wide ring of a dielectric material between the edge of the heater disc and the sphere wall. This electrical insulation should reduce the pickup of the radio-frequency power by the sphere wall.

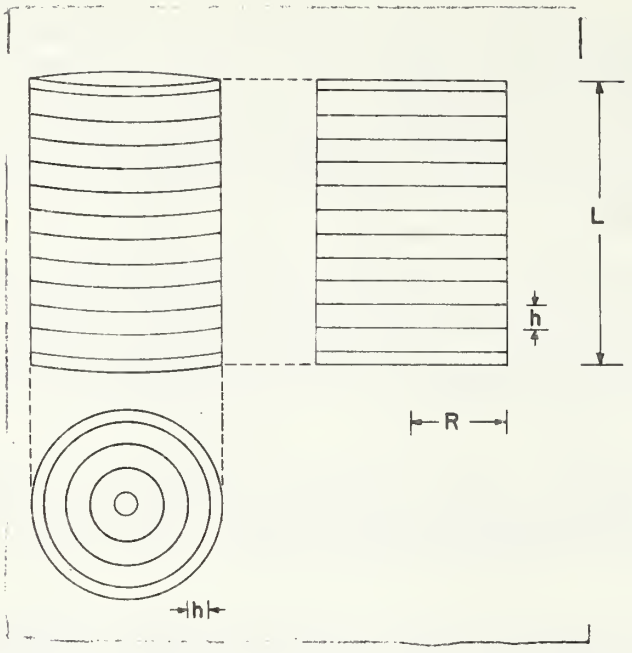

Figure 1. Cylindrical cavity with subdivided walls and base.

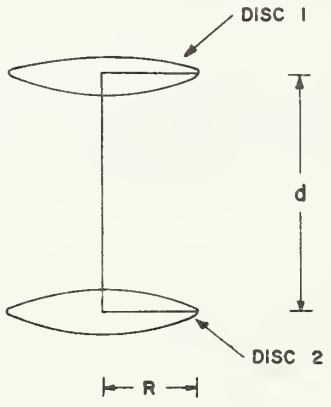

Figure 2. Coaxial discs of equal radii.

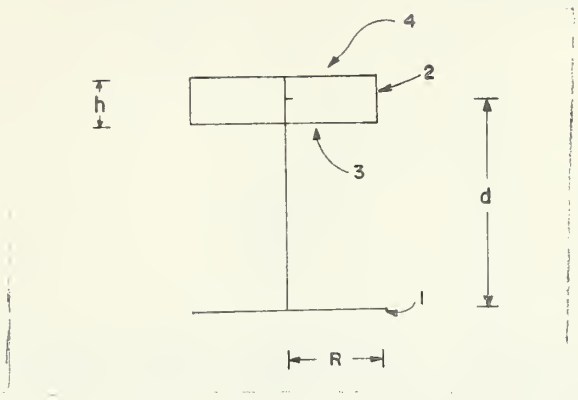

Figure 3. Section through a cylindrical cavity; areas 1, 3, and 4 are discs stretched across the cavity; area 2 is a cylindrical ring on the cavity wall.

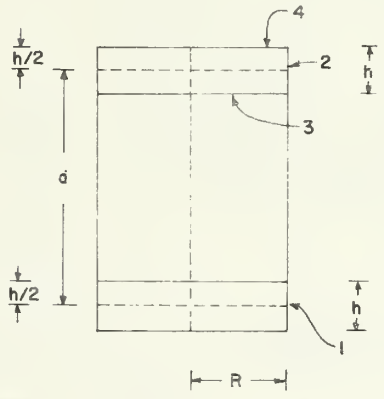

Figure 4. Section through a cylindrical cavity; areas 1 and 2 are cylindrical rings on the cavity wall; areas 3 and 4 are circular discs stretched across the cylinder.

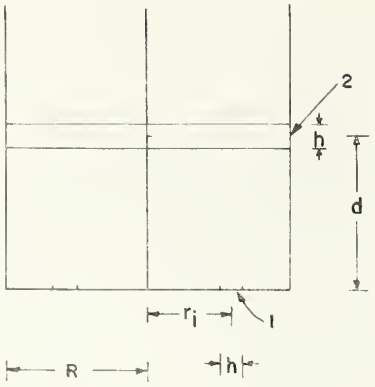

Figure 5. Section through a cylindrical cavity; area 1 is an annular ring on the base of the cavity; area 2 is a cylindrical ring on the cavity wall.

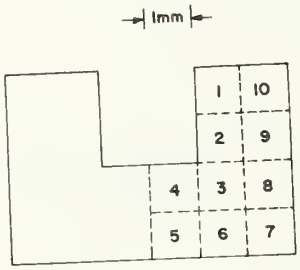

Figure 6. Cylindrical geometry used in trial calculation of heat transfer in a cavity.

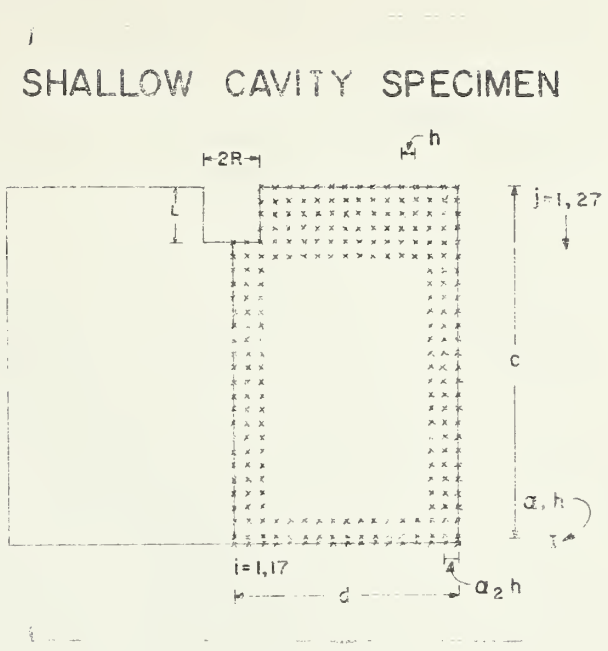

Figure 7. Cylindrical specimen of radius d and length c containing a shallow cylindrical cavity of radius R and length L; nodes are distributed evenly throughout the specimen except at the edge and base of the specimen.

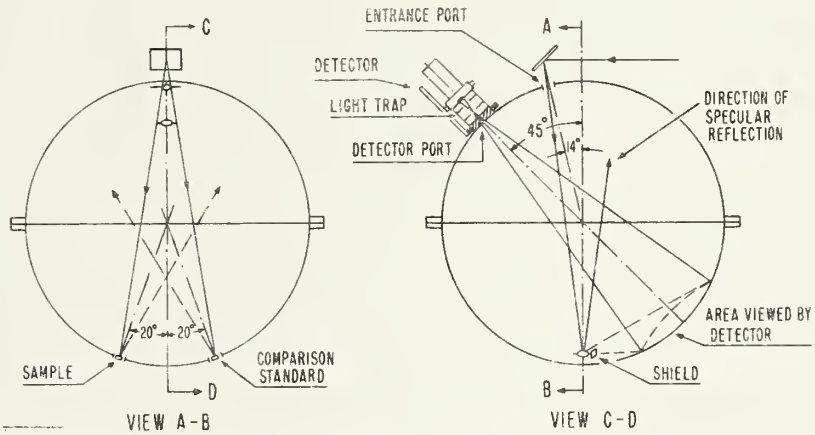

Figure 8. Schematic views of sphere geometry sectioned along the secondary plane of the sphere, view A-B, showing the location of sample and comparison standard ports, and sectioned along the primary plane of the sphere, view C-D, showing the location of entrance port, detector, area viewed by detector, and shields. The sphere is 14-in. in diameter. The line A-B or C-D is the principal axis of the sphere.


DEPARTMENT OF COMMERCE
NATIONAL BUREAU OF STANDARDS